SEUSS integrates transcriptional and epigenetic control of root stem cell organizer specification

Huawei Zhai[1,2,†], Xiaoyue Zhang[1,†] (iD), Yanrong You[1], Lihao Lin[3], Wenkun Zhou[4,5,*] (iD) & Chuanyou Li[1,2,**] (iD)

Abstract

Proper regulation of homeotic gene expression is critical for stem cell fate in both plants and animals. In *Arabidopsis thaliana*, the *WUSCHEL (WUS)-RELATED HOMEOBOX 5 (WOX5)* gene is specifically expressed in a group of root stem cell organizer cells called the quiescent center (QC) and plays a central role in QC specification. Here, we report that the SEUSS (SEU) protein, homologous to the animal LIM-domain binding (LDB) proteins, assembles a functional transcriptional complex that regulates *WOX5* expression and QC specification. SEU is physically recruited to the *WOX5* promoter by the master transcription factor SCARECROW. Subsequently, SEU physically recruits the SET domain methyltransferase SDG4 to the *WOX5* promoter, thus activating *WOX5* expression. Thus, analogous to its animal counterparts, SEU acts as a multi-adaptor protein that integrates the actions of genetic and epigenetic regulators into a concerted transcriptional program to control root stem cell organizer specification.

Introduction

Despite the huge evolutionary distance between plant and animal kingdoms, stem cell niches in both living forms contain organizer cells that maintain the adjacent stem cells (Dolan *et al*, 1993; Scheres, 2007; Dinneny & Benfey, 2008). In the model plant *Arabidopsis thaliana*, root stem cells are maintained by a small group of slowly dividing organizer cells called the quiescent center (QC) (Aichinger *et al*, 2012; Petricka *et al*, 2012). The QC generates signals that prevent differentiation of abutting stem cells, and it also acts as a reservoir to replace injured stem cells (van den Berg *et al*, 1995; Xu *et al*, 2006; Cruz-Ramírez *et al*, 2013). In turn, the pluripotent stem cells undergo formative asymmetric division to generate specific tissue layers of the whole root system (Aichinger *et al*, 2012; Petricka *et al*, 2012). QC is first initiated in the embryo by asymmetric division of the hypophyseal cell during the early-to-mid-globular embryo stage; the upper lens-shaped daughter cell acquires QC identity, whereas the lower daughter cell becomes columella stem cells (CSCs) (Jürgens *et al*, 1994; Scheres & Benfey, 1999; Jürgens, 2001; Weigel & Jürgens, 2002). Remarkably, QC and the entire root stem cell niche can be readily re-established in response to internal cues and external stresses during the lifelong post-embryonic growth, which, as in the case of some trees, can extend beyond several thousand years (Chen *et al*, 2011; Marhava *et al*, 2019; Zhou *et al*, 2019).

Decades of molecular genetic studies have identified key transcription factors that regulate the acquisition of QC identity. Among these, the homeodomain transcription factor WUSCHEL (WUS)-RELATED HOMEOBOX 5 (WOX5) is the best-studied molecular marker of QC identity (Sarkar *et al*, 2007). *WOX5* expression coincides with the embryonic formation of QC progenitors and persists specifically in the QC during post-embryonic root growth (Haecker *et al*, 2004; Sarkar *et al*, 2007). WOX5 suppresses CYCLIN D activity to establish the quiescence of the QC and coordinates with several hormonal signals and transcriptional regulators to maintain the identity of CSCs (Stahl *et al*, 2009; Ding & Friml, 2010; Chen *et al*, 2011; Stahl *et al*, 2013; Forzani *et al*, 2014; Pi *et al*, 2015). Given that *WOX5* is exclusively expressed in the QC, extensive research has been conducted to identify factors that confine *WOX5* expression to such a narrow domain (Zhang *et al*, 2015; Long *et al*, 2017). However, the molecular mechanism underlying *WOX5* expression activation remains largely unknown.

In contrast to *WOX5*, which is expressed exclusively in the QC, genes encoding the SCARECROW (SCR)/SHORT ROOT (SHR)

1 State Key Laboratory of Plant Genomics, National Center for Plant Gene Research (Beijing), Institute of Genetics and Developmental Biology, Innovation Academy of Seed Design, Chinese Academy of Sciences, Beijing, China
2 CAS Center for Excellence in Biotic Interactions, University of Chinese Academy of Sciences, Beijing, China
3 State Key Laboratory of Crop Biology, College of Agronomy, Shandong Agricultural University, Tai'an, Shandong Province, China
4 State Key Laboratory of Plant Physiology and Biochemistry, College of Biological Sciences, China Agricultural University, Beijing, China
5 Frontier Science Center for Molecular Design and Breeding, China Agricultural University, Beijing, China
   *Corresponding author. Tel: +86 13426014658; E-mail: zhouwenkun@cau.edu.cn
   **Corresponding author (lead contact). Tel: +86 10 64806612; E-mail: cyli@genetics.ac.cn
   †These authors contributed equally to this work

transcription factors (belonging to the GRAS family) and PLETHORA (PLT) transcription factors [belonging to the APETALA2 (AP2) family] are expressed in larger domains including the QC (Di Laurenzio *et al*, 1996; Helariutta *et al*, 2000; Wysocka-Diller *et al*, 2000; Sabatini *et al*, 2003; Aida *et al*, 2004; Heidstra *et al*, 2004; Galinha *et al*, 2007). The *scr* single mutant and *plt1 plt2* double mutant displayed similar root stem cell defects (Sabatini *et al*, 2003; Aida *et al*, 2004), leading to the hypothesis that the SCR/SHR and PLT pathways converge to specify the QC identity as follows: The SCR/SHR pathway provides positional information along the radial axis, while the PLT pathway provides apical–basal information (Scheres, 2007; Dinneny & Benfey, 2008). Consistent with this hypothesis, a recent study proposed that PLT and SCR form a protein complex through their interaction with the teosinte-branched cycloidea PCNA (TCP) transcription factor, and the PLT–TCP–SCR complex is essential for *WOX5* expression and QC specification (Shimotohno *et al*, 2018). However, a previous study showed that the expression of *WOX5* was reduced or undetectable in *shr* and *scr* mutants, but expanded to regions abutting the QC in the *plt1 plt2* double mutant (Sarkar *et al*, 2007), suggesting that the SCR/SHR and PLT1/2 transcription factors might regulate *WOX5* expression via distinct modes of action.

The glutamine (Q)-rich SEUSS (SEU) protein contains a conserved domain, which shares high sequence similarity with the dimerization domain of the LIM-domain-binding (LDB) transcriptional co-regulator proteins in animals (Franks *et al*, 2002). The animal LDB proteins, such as LDB1 in mouse and Chip in *Drosophila*, play fundamental roles in the transcriptional regulation of cell-fate determination in versatile developmental processes (Agulnick *et al*, 1996; Morcillo *et al*, 1997; Matthews & Visvader, 2003; van Meyel *et al*, 2003; Bronstein *et al*, 2010; Bronstein & Segal, 2011; Love *et al*, 2014; Liu & Dean, 2019). Similar to its animal counterparts, SEU associates with cis-regulatory elements through its interaction with specific transcription factors to regulate gene expression during multiple developmental processes (Franks *et al*, 2002; Pfluger & Zambryski, 2004; Sridhar *et al*, 2004, 2006; Grigorova *et al*, 2011; Gong *et al*, 2016; Huai *et al*, 2018).

Here, we report that SEU assembles a transcriptional complex to regulate root stem cell-fate determination. SEU functions in the SCR signaling pathway to promote *WOX5* expression for QC specification. SCR physically interacts with and recruits SEU to the *WOX5* promoter. Then, SEU recruits the ASH1-RELATED 3 (ASHR3) methyltransferase SET DOMAIN GROUP 4 (SDG4) (Cartagena *et al*, 2008; Kumpf *et al*, 2014) to the *WOX5* promoter, which induces trimethylation of histone H3 lysine (K) 4 (H3K4me3), leading to *WOX5* expression activation. Thus, SEU plays a fundamental role in the cell-fate determination of root stem cell organizers by coordinating the formation of a functional SCR–SEU–SDG4 transcriptional complex.

Results

SEU positively regulates *WOX5* expression and QC specification

To investigate the role of SEU in root stem cell determination, we generated transgenic plants expressing *SEU* fused to the *green fluorescence protein* (*GFP*) gene under the control of the *SEU* promoter

(*pSEU::SEU-GFP*). The SEU-GFP fusion was localized to the nucleus and broadly expressed in the root meristem of post-embryonic seedlings (Fig EV1A). During embryogenesis, the expression of SEU-GFP was initiated early at the dermatogen stage and enriched broadly in different cells of the developing embryo (Fig 1A).

We then investigated the effect of SEU on the expression of *WOX5*, which is specifically expressed in and required for QC specification and function (Sarkar *et al*, 2007), by expressing the *pWOX5::GFP* construct (Blilou *et al*, 2005) in wild-type (WT) and *seu-3* mutant (Pfluger & Zambryski, 2004) plants. In WT embryos, *pWOX5::GFP* expression was initiated in the QC progenitors at the early globular stage (Fig 1A). However, in *seu-3* mutant embryos, *pWOX5::GFP* expression initiation was delayed to the heart stage, and the level of *pWOX5::GFP* expression was significantly reduced compared with the WT (Fig 1A and B).

At 5 days after germination (DAG), *seu-3* seedlings displayed markedly reduced *pWOX5::GFP* expression compared with the WT (Fig 1C–E). Consistently, reverse transcription-quantitative PCR (RT–qPCR) assays showed that the *WOX5* transcript levels were significantly reduced in *seu-3* seedlings compared with WT seedlings (Fig 1F). Together, these results indicate that SEU plays an essential role in promoting *WOX5* expression during both embryogenesis and post-embryonic development.

Next, we investigated whether the observed delay and reduction in *WOX5* expression in *seu-3* were accompanied by defects in QC specification and function. Similar to the *wox5-1* mutant (Sarkar *et al*, 2007), *seu-3* seedlings showed supernumerary cells with nonstereotyped shapes in the QC position (Fig 1C, D and G–I). Consistently, expression of the QC-specific marker *QC184* was markedly reduced in *seu-3* seedlings compared with the WT (Fig 1L and M), suggesting a loss of QC identity. The CSCs adjacent to the QC in *seu-3* seedlings were also abnormal in shape and size and showed ectopic accumulation of starch granules, indicating that they had undergone differentiation (Fig 1L and M). Consistently, expression of the CSC-specific marker *J2341* was largely abolished (Fig 1N and O), while that of the columella marker *CS9227* expanded to the CSCs (Fig 1P and Q). Complementation of the *seu-3* mutant by the introduction of the *pSEU::SEU-GFP* construct confirmed that the *seu-3* mutation caused the observed phenotype (Fig EV1A–D). Together, these observations revealed that SEU positively regulates *WOX5* expression and QC specification.

To determine the genetic relationship between *SEU* and *WOX5*, we generated a *seu-3 wox5-1* double mutant line. The *seu-3 wox5-1* double mutant exhibited similar QC defects and CSC differentiation phenotypes as the *wox5-1* mutant (Fig 1G–K). In addition, expression of *pWOX5::WOX5-GFP* (Pi *et al*, 2015) in *seu-3* partially rescued the QC defects of the mutant (Fig EV1E–G). These results collectively support that SEU acts in the same pathway with WOX5 to regulate QC specification.

SEU functions in the SHR/SCR pathway to promote *WOX5* expression and QC specification

Next, we asked whether and how SEU interacts with the master transcription factors SHR/SCR and PLTs, which converge in the root stem cell niche and play essential roles in QC specification (Sabatini *et al*, 2003; Aida *et al*, 2004; Scheres, 2007; Dinneny & Benfey, 2008). In the *scr-3* mutant embryo, the expression of the *pWOX5::*
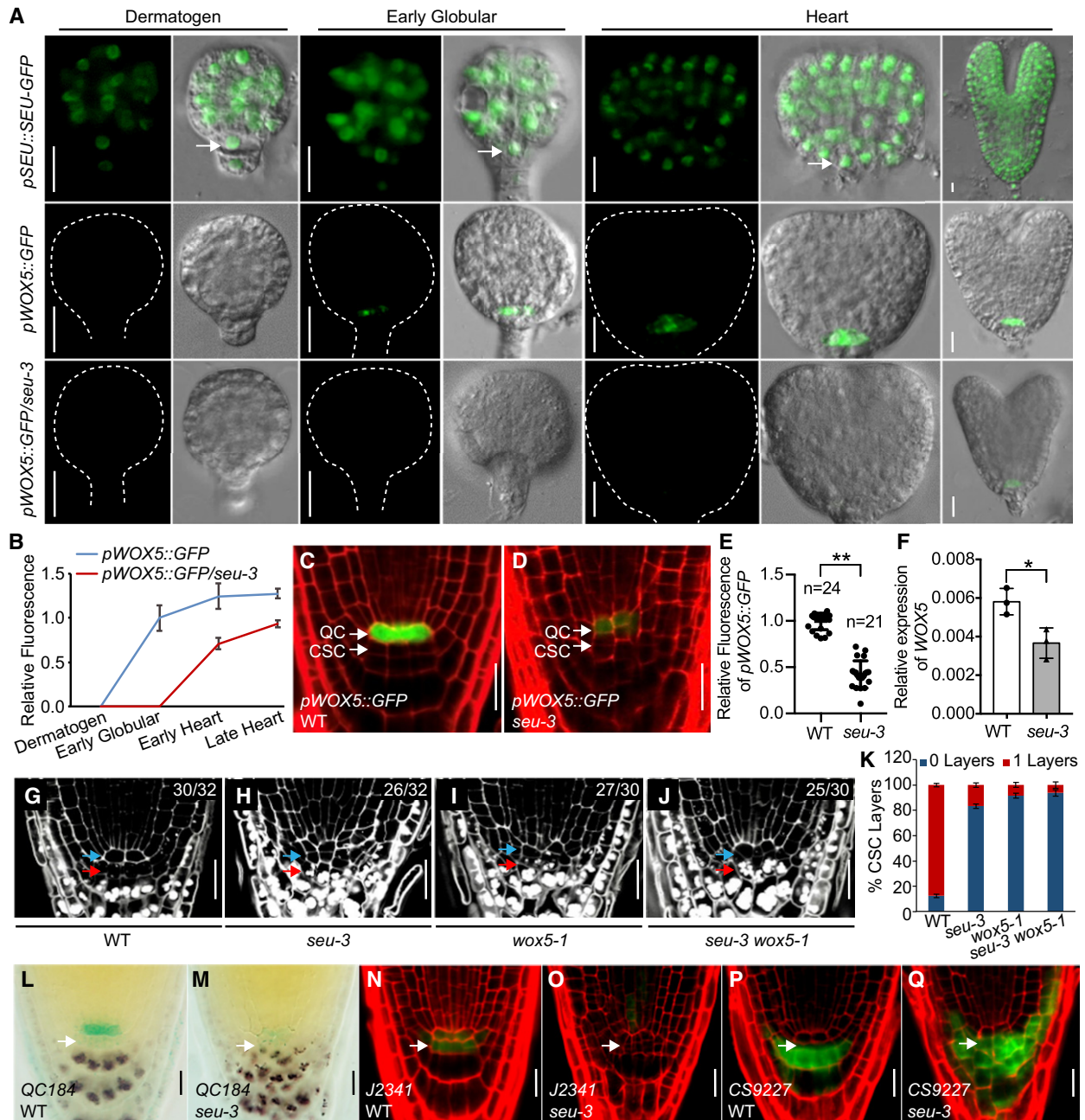
Figure 1. Ablation of SEU reduces *WOX5* expression and impairs quiescent center (QC) specification.

A   Expression patterns of *pSEU::SEU-GFP* and *pWOX5::GFP* in the embryos of the indicated genotypes at dermatogen, early globular, and heart stages. White arrows indicate the QC precursor cell, and white dashed lines indicate embryos. Scale bars: 10 μm.

B   Quantification of *pWOX5::GFP* GFP fluorescence in wild-type (WT) and *seu-3* mutant embryos. Fluorescence intensity at the early globular stage of WT embryos was set to 1.

C, D   Expression pattern of *pWOX5::GFP* in WT (C) and *seu-3* (D) embryos at 5 days after germination (DAG). Scale bars: 20 μm.

E   Quantification of GFP fluorescence in the QC of *pWOX5::GFP* transgenic plants, as shown in (C) and (D). Fluorescence intensity was normalized to the WT.

F   RT–qPCR analysis of the relative expression levels of *WOX5* in WT and *seu-3* roots. Total RNA was extracted from 5 mm root tip sections of seedlings at 5 DAG.

G–J   Modified pseudo-Schiff propidium iodide (mPS-PI) staining of stem cell niche areas in the indicated genotypes at 5 DAG. Blue arrows indicate the QC, and red arrows indicate the columella stem cells (CSCs). The numbers denote total number of scored samples, with similar phenotypes showing in (G–J). Scale bars: 20 μm.

K   Quantification of the CSC layer in the indicated genotypes at 5 DAG.

L, M   Double staining of the *QC184* β-glucuronidase (GUS) marker (light blue) and starch granules (dark brown) in WT (L) and *seu-3* (M) seedlings at 5 DAG.

N, O   Expression pattern of *J2341* in WT (N) and *seu-3* (O) seedlings at 5 DAG.

P, Q   Expression pattern of *CS9227* in WT (P) and *seu-3* (Q) seedlings at 5 DAG.

Data Information: In (B), (E), (F), and (K), data represent mean ± SD of three independent replicates. *n* denotes the total number of scored samples. Individual values (black dots) are shown. **$P < 0.01$, *$P < 0.05$ (Student's *t*-test). In (L–Q), white arrows indicate the CSCs. Scale bars: 20 μm.

Figure 2. SEU acts in the SHR/SCR pathway to promote *WOX5* expression and QC specification.

A–C Expression pattern of *pWOX5::GFP* in WT (A), *scr-3* (B), and *plt1-4 plt2-2* (C) at 5 DAG.
D Quantification of GFP fluorescence in the QC of *pWOX5::GFP* transgenic seedlings, as shown in (A–C). GFP signal intensity in each genotype was normalized relative to that in the WT.
E RT–qPCR analysis of the relative expression levels of *WOX5* in WT, *scr-3*, and *plt1-4 plt2-2* roots. Total RNA was extracted from 5 mm root tip sections of seedlings at 5 DAG.
F Primary root length of the indicated genotypes at 5 DAG.
G–J Representative confocal images of the indicated genotypes at 5 DAG. White arrows indicate the QC.
K Quantification of GFP fluorescence in the QC of *pSCR::GFP* and *pSCR::GFP-SCR* transgenic seedlings, as shown in (G–J). GFP signal intensity of each genotype was normalized relative to that of the WT.
L–Q Root stem cell niche phenotypes of the indicated genotypes at 5 DAG. White dashed lines indicate the QC region. The numbers denote total number of scored samples, with similar phenotypes showing in (L–Q).

Data information: In (D), (F), and (K), *n* denotes the total number of scored samples. Individual values (black dots) are shown. Data represent mean ± SD of three independent replicates. In (D) and (F), different lowercase letters indicate significant differences by one-way ANOVA followed by Tukey's multiple comparison test (*P* < 0.01). In (E) and (K), **P < 0.01 (Student's *t*-test). Scale bars: 20 μm.

GFP construct did not initiate until the heart stage, and the level of *pWOX5::GFP* expression was significantly lower than that in the WT embryo (Fig EV2A and B). By contrast, the *plt1-4 plt2-2* double mutant showed higher *pWOX5::GFP* expression compared with the WT (Fig EV2A and B). Similarly, at 5 DAG, *pWOX5::GFP* expression was strongly reduced in *scr-3* seedlings compared with the WT (Fig 2A, B and D) but expanded to the CSCs surrounding the QC in *plt1-4 plt2-2* double mutant seedlings (Fig 2A, C and D). Consistently, RT–qPCR assays showed that the *WOX5* transcript levels were significantly reduced in the *scr-3* mutant but increased in the *plt1-4 plt2-2* double mutant compared with the WT (Fig 2E). These observations uncovered that, similar to SEU, SCR positively regulates *WOX5* expression, whereas PLT1/2 negatively regulate *WOX5* expression.

The finding that both SEU and SCR promote *WOX5* expression suggests that these proteins function in the same pathway. To test this possibility, we investigated the genetic interaction between SEU and SCR by comparing the root growth defects of the *seu-3 scr-3*

double mutant with its parental lines. While the *seu-3 scr-3* double mutant displayed similar root growth defects as the *scr-3* single mutant, *seu-3* significantly enhanced the root growth defects of the *plt1-4 plt2-2* (Fig 2F), indicating that *SEU* and *SCR* act genetically in the same pathway, which is independent of the PLT pathway. Consistent with these results, the expression of *pSCR::GFP-SCR* and *pSCR::GFP* was dramatically reduced in the QC region of *seu-3* roots (Fig 2G–K), revealing that mutation of the *SEU* gene leads to a significant reduction in *SCR* expression in the QC, which affects QC identity. We also observed reduced expression of *pSHR::GFP* and *pSHR::SHR-GFP* in *seu-3* roots compared with WT (Fig EV2D–G). Consistently, RT–qPCR assays showed that the *SHR* transcript levels were reduced in the *seu-3* mutant (Fig EV2C). These results are in line with recent observations that SEU acts as an upstream transcriptional regulator of *SHR* (Gong *et al*, 2016; Clark *et al*, 2020). The *seu-3 shr-2* double mutant displayed comparable root growth defects as *shr-2* (Fig 2F). Additionally, the QC defects observed in the *seu-3 scr-3* and the *seu-3 shr-2* double mutants were similar to

those observed in their parental lines, *scr-3* and *shr-2*, respectively (Fig 2L–Q). Together, our results support that SEU acts in the SHR/SCR pathway to regulate QC specification.

SCR physically recruits SEU to promote *WOX5* expression and QC specification

The finding that SEU and SHR/SCR functionally and genetically interact to regulate *WOX5* expression and QC specification prompted us to test their possible physical interaction. Yeast two-hybrid (Y2H) assays showed that SEU interacts with SCR (Fig 3A) but not SHR (Fig EV2H). To confirm this observation, we performed *in vitro* pull-down experiments using purified maltose-binding protein (MBP)-tagged SEU (SEU-MBP) and FLAG epitope-tagged SCR (SCR-FLAG) or SHR (SHR-FLAG). SEU-MBP pulled down SCR-FLAG but not SHR-FLAG (Fig 3B), indicating that SEU interacts specifically with SCR *in vitro*. Furthermore, in co-immunoprecipitation (Co-IP) experiments performed in *Nicotiana benthamiana* leaves, GFP-tagged SCR (SCR-GFP) was immunoprecipitated by SEU-myc (Fig 3C). In Co-IP assays performed in transgenic *Arabidopsis* plants expressing *SCR-GFP* using anti-SEU antibody, SCR-GFP pulled down endogenous SEU (Fig 3D), confirming that SEU interacts with SCR *in planta*.

The above results suggest that SEU is physically recruited by SCR to the *WOX5* promoter to promote its expression. Consistent with this presumption, chromatin immunoprecipitation (ChIP)-qPCR assays using *pSCR::GFP-SCR* transgenic *Arabidopsis* plants and anti-GFP antibody showed the enrichment of *WOX5* promoter at approximately −1,100 bp (Fig 3E, fragment B and 3F). Parallel ChIP-qPCR assays using *pSEU::SEU-GFP* transgenic *Arabidopsis* roots and anti-GFP antibody revealed a similar enrichment pattern of the *WOX5* promoter as that obtained using *pSCR::GFP-SCR* plants (Fig 3E, fragment B and 3G). Together, these results indicate that SEU and SCR are recruited to the same region of the *WOX5* promoter. However, in *scr-3* mutant plants expressing the *pSEU::SEU-GFP* construct, the enrichment of the *WOX5* promoter was markedly reduced (Fig 3E, fragment B and 3H), indicating that the recruitment of SEU on the *WOX5* promoter is dependent on SCR.

Next, we used a dual-luciferase (LUC) reporter system (Hellens *et al*, 2005) to examine the effect of SCR on *WOX5* expression. To perform this experiment, a 3,100 bp fragment of the *WOX5* promoter was cloned into the dual-LUC reporter system to generate a *pWOX5::LUC* reporter construct (Fig 3I). Co-expression of *SCR* with *pWOX5::LUC* in *N. benthamiana* leaves increased LUC activity, confirming that SCR positively regulates *WOX5* expression (Fig 3I). When *SEU* and *SCR* were coexpressed with the *pWOX5::LUC* reporter, LUC activity was significantly enhanced further (Fig 3I), indicating that SEU acts as a co-activator of SCR in regulating *WOX5* expression.

We then asked whether QC-enriched expression of *SEU* or *SCR* could rescue the *WOX5* expression and QC defects of the *seu* mutant. For this purpose, we introduced the *pWOX5::SEU-GFP* construct or the *pWOX5::SCR-GFP* construct into the *seu-3* mutant. As expected, the *pWOX5::SEU-GFP* construct restored *WOX5* promoter activity and rescued the QC defects of the *seu-3* mutant (Fig 3J, K and N). By contrast, the *pWOX5::SCR-GFP* construct failed to rescue the *WOX5* expression and QC defects of the mutant (Fig 3L–N). Taken together, these results demonstrate that the

transcriptional co-regulator SEU is physically recruited by SCR to promote *WOX5* expression and QC specification.

SEU recruits SDG4 to induce methylation of the *WOX5* promoter

To understand how SEU co-activates *WOX5* expression along with SCR, we performed Y2H assays to identify SEU-interacting proteins. In a Y2H screen, we found that the histone methyltransferases SDG4 and SDG25 interact with SEU (Figs 4A and EV3A). To determine whether SDG4 and SDG25 interact with SEU *in planta*, we conducted firefly LUC complementation imaging (LCI) assays (Chen *et al*, 2008) using *N. benthamiana* leaves. *SDG4* was fused to the C-terminal half of *LUC* (*cLUC-SDG4*), while *SEU* was fused to the N-terminal half of *LUC* (*SEU-nLUC*). Co-expression of *cLUC-SDG4* and *SEU-nLUC* constructs in *N. benthamiana* cells resulted in a strong fluorescence signal, indicating that SDG4 interacts with SEU in plant cells (Fig EV3B). Parallel experiments indicated that SDG25 also interacts with SEU in plant cells (Fig EV3C).

We then asked the functional relevance of SEU interaction with SDG4 and SDG25 in regulating QC specification. In line with previous observations (Kumpf *et al*, 2014), the *ashr3-1* mutant, which contains a T-DNA insertion in the *SDG4* gene, exhibited aberrant cellular organization in the QC and differentiated CSCs, similar to the *seu-3* mutant (Fig 4J and L). In comparison with *ashr3-1*, the *sdg25-1* mutant (Berr *et al*, 2009; Tamada *et al*, 2009) displayed relatively weaker defects in the QC and CSC (Fig EV3D–F), we therefore focused on SDG4 to investigate its role in regulating *WOX5* expression and QC specification by using transgenic plants expressing the *pSDG4::SDG4-GFP* construct. During embryogenesis, the SDG4-GFP fusion protein was expressed in the hypophyseal cell at the dermatogen stage (Fig EV3G), and during post-embryonic root development, SDG4-GFP was strongly expressed in the root meristem (Fig EV3H). ChIP-qPCR experiment revealed that SDG4 indeed associated with the same region of the *WOX5* promoter as SCR and SEU (Fig 4B, fragment B, C, compared to Fig 3E–G, fragment B; and Fig EV4A). Previous studies indicated that SDG4-mediated histone H3 methylation is involved in diverse physiological processes including pollen tube growth and pathogen-responsive gene expression (Cartagena *et al*, 2008; De-La-Pena *et al*, 2012). Our ChIP-qPCR analyses revealed that the level of H3K4me3 modification in the *WOX5* promoter was significantly decreased, whereas the level of H3K4me2 modification in the *WOX5* promoter was slightly increased in the *ashr3-1* mutant as compared to the WT (Figs 4B and D, and EV4B). In parallel ChIP-qPCR experiments, we found that the levels of H3K36me and the H3K36me3 in the *WOX5* promoter of *ashr3-1* were comparable to those of WT (Fig EV4C and D). Consistently, the level of H3K4me3 modification in the *WOX5* promoter, but not the H3K4me modification and the H3K4me2 modification in the *WOX5* promoter, was significantly reduced in the *seu-3* mutant as compared to the WT (Figs 4E, and EV4E and F). Together, these results suggest that SEU physically recruits SDG4 to the *WOX5* promoter, which deposits the H3K4me3 mark.

Considering that H3K4me3 is associated with gene activation (Cheng *et al*, 2020), we predicted that the reduced level of H3K4me3 modification in the *WOX5* promoter in *ashr3-1* is correlated with decreased *WOX5* expression and defective QC
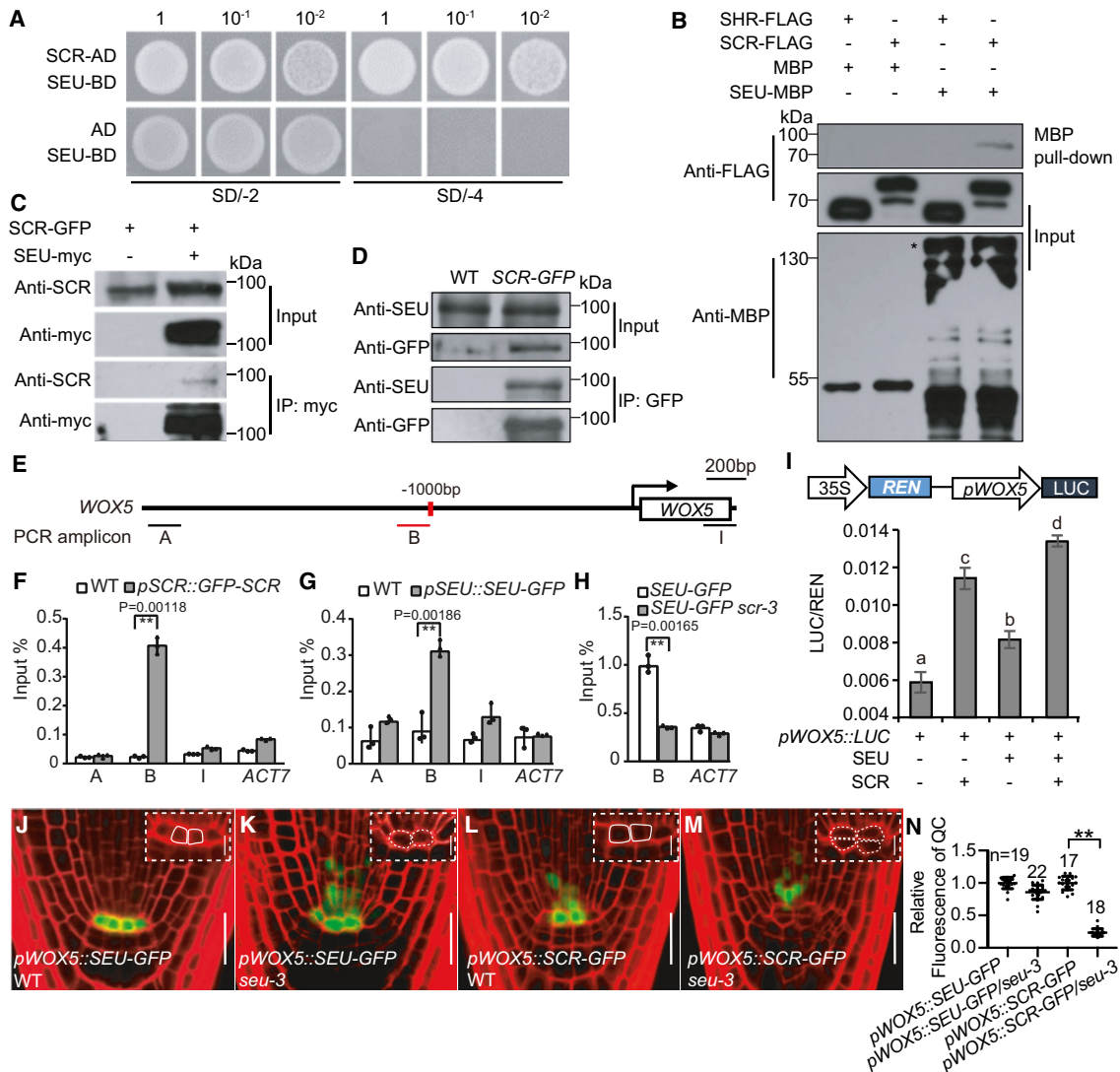
Figure 3. SCR recruits SEU to the *WOX5* promoter to promote its expression.

A   Yeast two-hybrid (Y2H) assays showing the interaction between SEU and SCR. The yeast transformants were plated on synthetic defined (SD) media lacking Leu and Trp (SD/-2) or lacking Ade, His, Leu, and Trp (SD/-4) to assess protein–protein interactions. AD, GAL4 activation domain; BD, GAL4 DNA-binding domain.

B   *In vitro* pull-down assays showing that SEU directly interacts with SCR but not with SHR. SCR-FLAG was pulled down by SEU-MBP immobilized on amylose resin. Protein bound to the amylose resin was eluted and analyzed by immunoblotting using anti-FLAG antibody. The asterisk indicates the position of SEU-MBP.

C   Verification of *in vivo* interactions between SCR and SEU in *Nicotiana benthamiana* leaves via Co-IP assays. SCR-GFP and SEU-myc were transiently coexpressed in *N. benthamiana* leaves. Protein samples were immunoprecipitated using anti-myc antibody.

D   Co-IP assays of SEU with SCR in *Arabidopsis*. Protein extracts from WT and *SCR-GFP* roots were isolated at 5 DAG and immunoprecipitated with anti-GFP antibody.

E   Schematic diagram of the *WOX5* and PCR amplicons (indicated as letters A, B, and I) used for ChIP-qPCR. TSS, transcription start site.

F, G   SCR and SEU physically bind to the *WOX5* promoter, as shown by ChIP-qPCR analysis. Chromatin was isolated from 5 mm root tip sections of seedlings at 5 DAG, sonicated, and immunoprecipitated using anti-GFP antibody. The precipitated DNA was used as a template for qPCR analysis. A, B, and I indicated the PCR amplicons as shown in (E). *ACT7*, control.

H   Mutation of the *SCR* gene impairs the recruitment of SEU to the *WOX5* promoter, as shown by ChIP-qPCR analysis. Chromatin was extracted from *SEU-GFP* and *SEU-GFP scr-3* seedlings at 5 DAG and precipitated with anti-GFP antibody. ChIP signals were quantified by qPCR as a percentage of total input DNA.

I   SEU stimulated SCR-mediated *WOX5* promoter activation in transient expression assays in *Nicotiana benthamiana* leaves. The *pWOX5::LUC* reporter was cotransformed with the indicated effector constructs. The *pWOX5::LUC* activity was normalized relative to the internal control [LUC/Renilla luciferase (REN)]. The schematic diagram shows the construct used in the transient expression assays. Arrows indicate promoter regions, and boxes indicate coding sequences. Different lowercase letters indicate significant differences by one-way ANOVA followed by Tukey's multiple comparison test (*P* < 0.01).

J–M   Representative confocal images of the indicated genotypes at 5 DAG. Scale bars: 20 μm. Insets show the QC region in which the solid white lines indicate the QC of WT, and the dashed white lines indicate the QC of *seu-3*. Insets scale bars: 5 μm.

N   Quantification of GFP signal intensity in the QC of WT and *seu-3* seedlings expressing *pWOX5::SEU-GFP* and *pWOX5::SCR-GFP*. GFP signal intensity in *seu-3* seedlings was normalized relative to the WT. Individual values (black dots) are shown. *n* denotes the total number of scored samples.

Data information: In (F), (G), (H), (I), and (N), data represent mean ± SD of three independent replicates. **P* < 0.01 (Student's *t*-test).
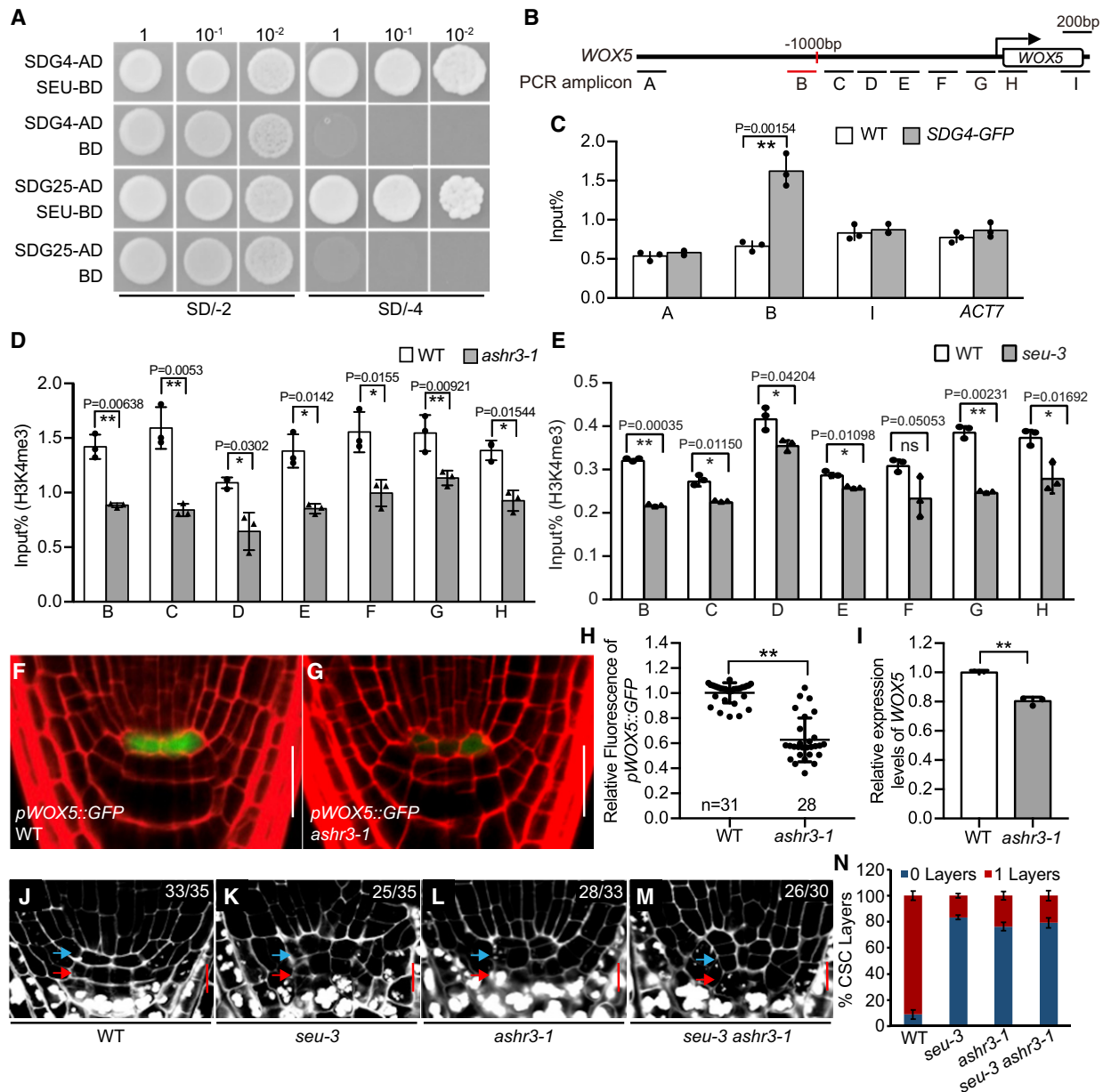Source data are available online for this figure.

Figure 4. SDG4 interacts with SEU and deposits H3K4me3 modification in the *WOX5* promoter.

A   Y2H assays showing that SEU interacts with SDG4 and SDG25. The yeast transformants were plated on SD/-2 and SD/-4 media to assess protein–protein interactions.

B   Schematic diagram of the *WOX5* and PCR amplicons (indicated as letters A–I) used for ChIP-qPCR.

C   SDG4 physically bind to the *WOX5* promoter, as shown by ChIP-qPCR analysis. *ACT7*, control.

D, E   ChIP-qPCR analysis indicating that mutations in *SDG4* and *SEU* genes impair H3K4me3 deposition in the *WOX5* promoter. ChIP signal was normalized to the WT. Individual values (black dots) are shown.

F, G   Expression pattern of *pWOX5::GFP* in the indicated genotypes at 5 DAG. Scale bars: 20 μm.

H   Quantification of GFP fluorescence in the indicated genotypes expressing *pWOX5::GFP*. GFP signal intensity in the WT was set to 1. *n* denotes the total number of scored samples.

I   RT–qPCR analysis of the relative expression levels of *WOX5* in WT and *ashr3-1* roots. Total RNA was extracted from 5 mm root tip sections of seedlings at 5 DAG. Individual values (black dots) are shown.

J–M   mPS-PI staining of stem cell niche in the indicated genotypes at 5 DAG. Blue arrows indicate the QC, and red arrows indicate the CSCs. The numbers denote total number of scored samples, with same phenotypes showing in (J–M). Scale bars: 10 μm.

N   Quantification of the CSC layer in the indicated genotypes at 5 DAG.

Data information: For (C–E), chromatin was isolated from 5 mm root tip sections of seedlings at 5 DAG, sonicated, and immunoprecipitated using anti-GFP or anti-H3K4me3 antibodies. The precipitated DNA was used as a template for qPCR analysis. PCR amplicons are shown in (B). In (C), (D), (E), (H), (I), and (N), data represent mean ± SD of three independent replicates. **$P < 0.01$, *$P < 0.05$ (Student's *t*-test).

specification. Indeed, the expression levels of *pWOX5::GFP* in *ashr3-1* were decreased to levels comparable to those in *seu-3* (Fig 4F–H, compared with Fig 1C–E). Consistently, RT–qPCR results showed that the *WOX5* transcript levels were significantly reduced in *ashr3-1* root tips compared with WT root tips (Fig 4I). Additionally, the *seu-3 ashr3-1* double mutant exhibited aberrant cellular organization in the QC and differentiated CSCs, similar to the *seu-3* mutant (Fig 4J–N). Collectively, these biochemical and genetic data support our finding that SEU physically recruits SDG4 to the *WOX5* promoter to regulate *WOX5* expression and QC specification.

SEU coordinates the formation of the SCR-SEU-SDG4 transcriptional complex *in planta*

To determine the genetic relationship among *SDG4*, *SEU*, and *SCR* in regulating *WOX5* expression and QC specification, we generated *ashr3-1 seu-3 wox5-1* and *ashr3-1 seu-3 scr-3* triple mutants (Fig 5A–G). The QC defects in *ashr3-1 seu-3 wox5-1* and *ashr3-1 seu-3 scr-3* triple mutants were similar to those observed in the *wox5-1* and *scr-3* single mutants, respectively (Fig 5D–G), corroborating that both SEU and SDG4 regulate *WOX5* expression and QC specification through the SCR signaling pathway. Next, we transformed *35S::*
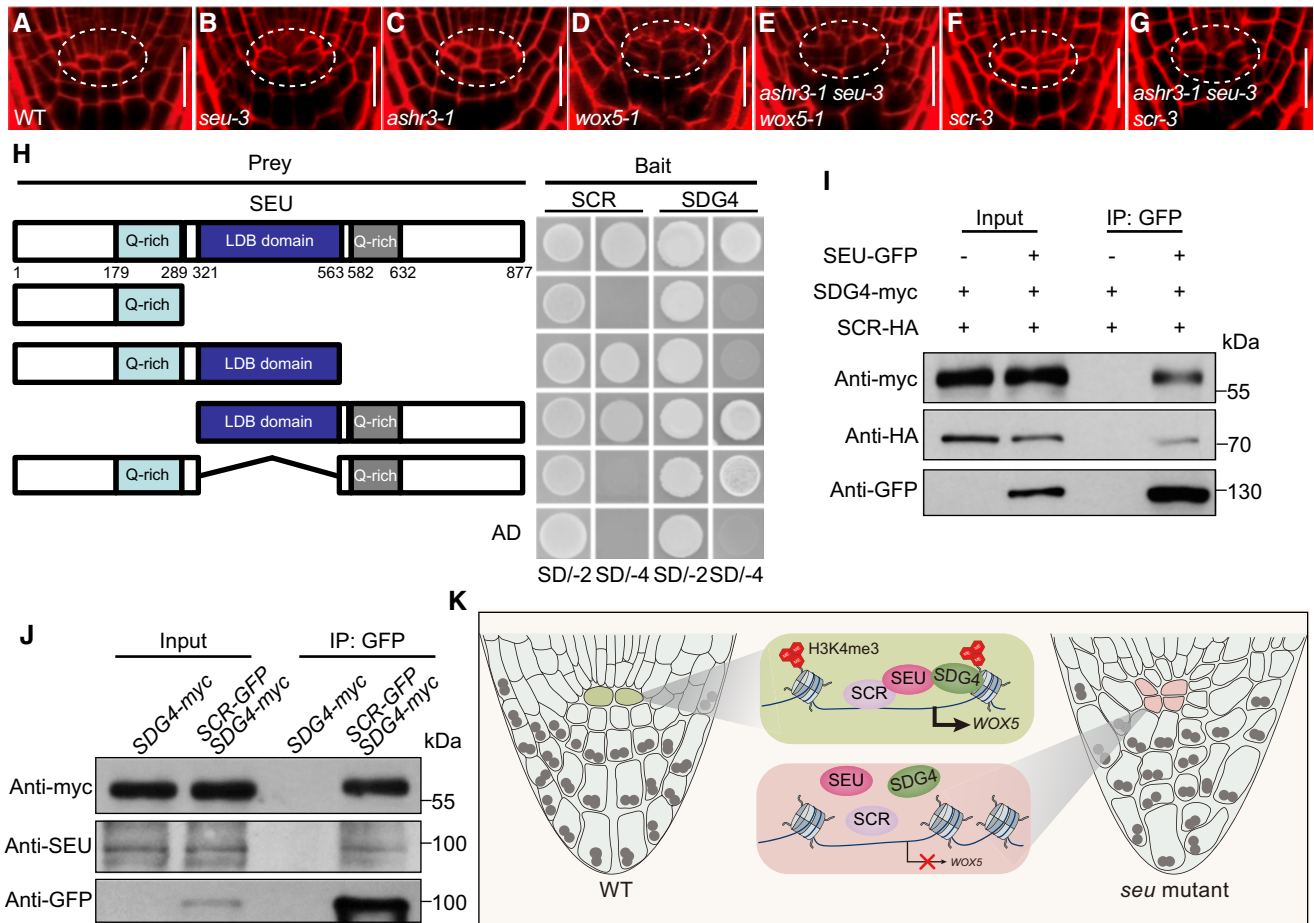

Figure 5. SEU cooperates with SCR and SDG4 to promote *WOX5* expression and QC specification.

A–G Representative confocal images of the indicated genotypes at 5 DAG. The white dashed lines indicate the QC region. Scale bars: 20 μm.

H Domain mapping of SEU involved in interactions with SCR and SDG4. The yeast transformants were plated on SD/-2 and SD/-4 media to assess protein–protein interactions.

I SEU associates with SCR and SDG4 in *Nicotiana benthamiana* leaves, as shown by Co-IP assays. *SDG4-myc*, *SCR-HA*, and *SEU-GFP* were coinfiltrated into *Nicotiana benthamiana* leaves. Protein samples were immunoprecipitated with anti-GFP antibody and immunoblotted with anti-myc and anti-HA antibody. *Nicotiana benthamiana* leaves coinfiltrated with *SDG4-myc* and *SCR-HA* were used as a negative control.

J Co-IP assays of SCR with SEU and SDG4 in *Arabidopsis*. Proteins extracted from *SDG4-myc* and *SDG4-myc SCR-GFP* plants were immunoprecipitated using anti-GFP antibody and immunoblotted using anti-myc and anti-SEU antibodies.

K Schematic representation of the role of SEU in SCR-mediated activation of *WOX5* expression. In WT roots, SEU is recruited to the promoter of *WOX5* through the SEU–SCR interaction. SEU interacts with SDG4, which promotes H3K4me3 deposition in the *WOX5* promoter. The SCR–SEU–SDG4 ternary complex plays an essential role in activating *WOX5* expression and QC specification. Mutation of *SEU* impairs the formation of the SCR–SEU–SDG4 complex, which leads to dramatically reduced *WOX5* expression and defective QC identity.

Source data are available online for this figure.

WOX5-GFP into *ashr3-1 seu-3 scr-3* plants and observed that the *35S::WOX5-GFP* construct was able to complement the QC defects of the *ashr3-1 seu-3 scr-3* triple mutant in a dosage-dependent manner (determined by *35S::WOX5-GFP* fluorescence signals) (Fig EV5), further confirming that SEU together with SCR and SDG4 function through WOX5 to control QC activity.

Since SEU physically interacts with both SCR and SDG4, we mapped the protein domains of SEU involved in these interactions. Y2H assays revealed that the LDB domain of SEU interacts with SCR, whereas the C-terminal Q-rich domain of SEU interacts with SDG4 (Fig 5H), indicating that SEU interacts with SCR and SDG4 via distinct domains. To determine whether SEU coordinates the formation of the SCR–SEU–SDG4 transcriptional complex *in planta*, we performed Co-IP assays using *N. benthamiana* leaves co-expressing *SEU-GFP*, *SDG4-myc*, and *SCR-HA*. Both SDG4-myc and SCR-HA could be pulled down by SEU-GFP (Fig 5I). Furthermore, in Co-IP experiments using transgenic plants expressing *SDG4-myc* and *SCR-GFP*, both SDG4-myc and endogenous SEU could be pulled down by SCR-GFP (Fig 5J), confirming the existence of the SCR–SEU–SDG4 complex in *planta*. In summary, our results suggest that SEU functions as a scaffold protein to orchestrate the formation of the SCR–SEU–SDG4 transcriptional complex, which regulates *WOX5* expression during QC specification (Fig 5K).

Discussion

SEU acts as an integrative hub to mediate QC specification and root patterning

The transcriptional program that determines stem cell fate in plants, as in animals, is controlled by a small number of master transcription factors. Previous studies suggest that master transcription factor-mediated protein–protein interaction networks play an important role in maintaining the QC-specific expression of *WOX5* (Long *et al*, 2017; Shimotohno *et al*, 2018). However, the exact mode of action of specific master transcription factors and the mechanism underlying the regulation of *WOX5* expression by these transcription factors remain elusive. Here, we show that whereas SCR promotes *WOX5* expression, PLT1/2 might negatively regulates *WOX5* expression. We demonstrate a mechanism whereby SEU assembles a functional SCR–SEU–SDG4 transcription complex to activate *WOX5* expression. At the *WOX5* promoter, SCR physically recruits SEU, which then physically recruits the epigenetic co-activator SDG4 to activate the expression of *WOX5* (Fig 5K). Interestingly, a *35S::WOX5-GFP* construct was able to complement the QC defects of the *ashr3-1 seu-3 scr-3* triple mutant (Fig EV5), suggesting that SEU together with SCR and SDG4 function through WOX5 to control QC activity. Our model highlights the mechanistic function of SEU as an interface that physically and functionally integrates master transcription factors and epigenetic regulators into a functional complex, which accurately regulates the transcription of genes controlling plant development.

Deposition of appropriate epigenetic marks is important for transcriptional regulation. Previous studies report that SDG4/ASHR3 is required for QC quiescence maintenance (Kumpf *et al*, 2014). They also reveal that SDG4 associates with H3K36me (Kumpf *et al*, 2014). Interestingly, we found that the levels of H3K36me and the

H3K36me3 modification in the *WOX5* promoter of WT and the *ashr3-1* mutant were comparable (Fig EV4C and D), but the level of H3K4me3 modification in the *WOX5* promoter was significantly reduced in the *ashr3-1* mutant compared with the WT (Fig 4B and D), suggesting that SDG4 associates to H3K4me3 in the *WOX5* promoter. The reduction in H3K4me3 on the *WOX5* promoter could be explained as an effect of reduced expression, or genome-wide down-regulation. To exclude these possibilities, we examined the effect of the *ashr3-1* mutation on the deposition of H3K4me3 in the promoter of a group of genes richly expressed in the root meristem including *PLT1*, *PLT2*, *PIN1*, *PIN3*, and *PIN4*. Results showed that the levels of H3K4me3 modification in the transcriptional start site of these genes were comparable between *ashr3-1* and WT (Fig EV4G), indicating that the reduction in H3K4me3 on the *WOX5* promoter may not be due to genome-wide down-regulation. In addition, it was reported that *SDG4* is a direct target of E2Fa/E2Fb transcription factors that control G1-to-S-phase transition (Kumpf *et al*, 2014). As WOX5 binds to promoters of D-type cyclins *CYCD3;3* and *CYCD1;1* and represses their expression in the QC (Forzani *et al*, 2014), it is of significance in future studies to explore the functional relevance of SDG4 and WOX5 in regulating QC activity with respect to cell-cycle regulation.

Notably, we found that the mutation of the *SEU* gene reduces *SCR* expression in the QC (Fig 2G–K), indicating that the SEU-dependent transcriptional complex, SCR–SEU–SCR, positively regulates the expression of *SCR*. This suggests that SEU operates a positive feedback loop to activate and maintain *WOX5* expression. In addition, during embryogenesis, *SCR*, *SEU*, and *SDG4* were expressed earlier than *WOX5*, suggesting that the SCR–SEU–SDG4 complex is important for the initiation of the QC progenitor hypophyseal cell.

Besides regulating QC specification, SCR, and its interacting partners, SHR and MED31, also regulate root ground tissue patterning (Di Laurenzio *et al*, 1996; Helariutta *et al*, 2000; Zhang *et al*, 2018). It was shown that SEU regulates the expression of *SCR* and *SHR*, thus playing an important role in the post-embryonic formation of the middle cortex in the ground tissue (Gong *et al*, 2016). Together, these observations suggest that, in addition to regulating QC specification, the SCR–SEU interaction module likely operates in other SHR/SCR-directed developmental programs. Indeed, it was proposed very recently that SEU is involved in a protein complex that acts as an upstream regulator of SHR and SCR, thereby differentially regulating the division timing of distinct cell types of the root stem cell niche (Clark *et al*, 2020).

Considering that SEU interacts with SCR and SDG4 through distinct protein domains, it is plausible that SEU provides a flexible interface to physically recruit and integrate versatile transcription factors and their co-factors to form linage-specific transcriptional programs that drive cell-fate determination and differentiation. Future studies are needed to identify these SEU-dependent transcriptional programs controlling root patterning.

SEU is an evolutionarily conserved transcriptional adaptor of cell-fate specification

Although we showed that SEU positively regulates *WOX5* expression, SEU was first identified for its repressive effect on the expression of the floral homeotic gene *AGAMOUS* (*AG*) (Franks *et al*, 2002). SEU represses *AG* expression by physically interacting with LUNIG (LUG), a transcriptional co-repressor containing a LUFS (LUG/LUH, Flo8,

and SSBP/SSDP) domain, which is highly conserved in the Groucho (Gro)/Tup1 family of co-repressors, including the mammalian single-stranded DNA-binding proteins (SSBPs, also known as SSDP in *Drosophila*) (Franks *et al*, 2002; van Meyel *et al*, 2003; Sridhar *et al*, 2004; Liu & Karmarkar, 2008). Notably, the LUFS domain of LUG is necessary and sufficient for its interaction with SEU (Sridhar *et al*, 2004; Liu & Karmarkar, 2008). Although the entire SEU protein is required for SEU–LUG interaction, SEU does contain a LDB1/Chip conserved domain (LCCD), which is essential for the interaction of LDB proteins with the LUFS domain of SSBPs (van Meyel *et al*, 2003; Sridhar *et al*, 2004; Bao *et al*, 2010). Analogous to the SEU–LUG interaction in plants, the LCCD–LUFS-mediated interactions between LDB proteins and SSBPs play critical roles in the transcriptional regulation of cell-fate decisions in diverse developmental systems including cardiogenesis, neurogenesis, and hematopoiesis (Matthews & Visvader, 2003; van Meyel *et al*, 2003; Love *et al*, 2014; Liu & Dean, 2019). The intriguing conservation of the LCCD–LUFS-mediated adaptor–co-repressor interactions across plants and vertebrates suggests that a fundamentally important protein–protein interaction mechanism enables regulated control of gene transcription. It is likely that plant- or animal-specific transcription regulators recruited this ancient transcription regulatory mechanism to mediate cell-fate determination and organ patterning.

Materials and Methods

Plant material and growth conditions

Arabidopsis thaliana ecotypes Columbia (Col-0), C24, and Landsberg *erecta* (L*er*) were used as the WT. Among the plant materials used in this study, the following were described previously: *QC25*, *QC46*, *QC184*, and *pSCR::GFP* (Sabatini *et al*, 1999); *pSCR::GFP-SCR* (Gallagher *et al*, 2004); *p35S::SCR-GFP* (Cruz-Ramirez *et al*, 2012); *pWOX5::GFP* (Blilou *et al*, 2005); *pWOX5::WOX5-GFP* (Pi *et al*, 2015); *pSHR::GFP* and *pSHR::SHR-GFP* (Nakajima *et al*, 2001); *seu-3* (Pfluger & Zambryski, 2004); *scr-3* (Fukaki *et al*, 1998); *shr-2* (Helariutta *et al*, 2000); *plt1-4 plt2-2* (Aida *et al*, 2004); and *wox5-1* (Sarkar *et al*, 2007). Seeds of *CS9227* and *J2341* were obtained from the Haseloff enhancer trap GFP line collection (http://www.plantsci.cam.ac.uk/Haseloff). Seeds of the *ashr3-1* (SAIL_804_D06) and *sdg25-1* (SALK_149692) mutants were obtained from the Arabidopsis Biological Resource Center (ABRC), Ohio, USA (http://www.arabidopsis.org/abrc/).

Seeds were surface-sterilized for 10 min in 10% commercial kitchen bleach, washed three times with sterile water, and plated on half-strength Murashige and Skoog (1/2MS) medium (Murashige & Skoog, 1962) supplemented with 1% sucrose and 0.8% agar. Plants were stratified in vertically or horizontally oriented Petri dishes at 4°C for 2 days in the dark and then transferred to a phytotron set at 22°C, 16 h light/8 h dark photoperiod, and 120 μmol photons/m^2/s light intensity. Roots of seedlings were examined at 3–5 DAG, depending on the experimental requirements.

Plasmid construction and plant transformation

To construct *pSEU::SEU-GFP* and *pSDG4::SDG4-GFP* plasmids, the *GFP* coding sequence (CDS) and *nopaline synthase* terminator

(*NOS-T*) sequence were amplified from the *pGFP-2* vector, and cloned in-frame at the 3′ end of the promoter and CDSs of *SEU* and *SDG4*, respectively, in the *pCAMBIA1300* binary vector using restriction endonucleases. To generate *pWOX5::SEU-GFP* and *pWOX5::SCR-GFP* constructs, the *WOX5* promoter and *SEU* and *SCR* CDSs were amplified by PCR and cloned into *pCAMBIA1300*-GFP (Zhang *et al*, 2018). To generate the *p35S::SEU-GFP* construct, the *SEU* CDS was PCR amplified and cloned into the *pENTR* vector using a pENTR Directional TOPO Cloning Kit (Invitrogen), and then recombined with the *PGWB5* binary vector containing the *GFP* CDS under the control of the cauliflower mosaic virus (CaMV) *35S* promoter. Primers used for plasmid construction are listed in Appendix Table S1.

Constructs were transformed into *Agrobacterium tumefaciens* strain GV3101 to generate transgenic *Arabidopsis* plants using the floral dip transformation method. Transformants were selected based on their resistance to hygromycin. Homozygous T3 or T4 lines were used to perform various experiments. The *p35S::SEU-GFP* construct was introduced into the *scr-3* mutant background by crossing, and homozygous plants were selected by genotyping.

Histology and microscopy

β-Glucuronidase (GUS) staining was performed as described previously (Zhou *et al*, 2010). Whole seedlings were immersed in the GUS staining solution [1 mM X-glucuronide in 100 mM sodium phosphate (pH 7.2), 0.5 mM ferricyanide, 0.5 mM ferrocyanide, and 0.1% Triton X-100], briefly vacuum-infiltrated, and incubated at 37°C in the dark for 1 h. Differential interference contrast (DIC) images were captured using the Leica DM5000B microscope. Images were processed using the Spot Flex software. Modified pseudo-Schiff propidium iodide (mPS-PI) staining was performed as described previously (Zhang *et al*, 2018). To perform confocal laser scanning microscopy, root tips of 3–5 DAG seedlings were stained with 10 μg/ml PI (Sigma P-4170) for 5 min and observed under a Zeiss LSM 710 confocal microscope system. PI staining and GFP signals were visualized at wavelengths ranging from 600–640 and 500–540 nm, respectively. Images were taken with the ZEN 2012 software (Zeiss). GFP signal intensity was quantified as described previously (Zhang *et al*, 2018). The same offset and gain settings were used for WT, *seu-3*, and *ashr3-1* seedlings, and the GFP signal was measured using the ZEN software on unmodified root images. At least 20 seedlings or embryos per genotype were observed.

Yeast two-hybrid (Y2H) assays

Y2H assays were based on the MATCHMAKER GAL4 Two-Hybrid System (Clontech). To verify the interaction between SCR and SEU, the CDS of *SCR* was fused to the GAL4 activation domain (AD) in *pGADT7*, and CDSs of *SEU* and its derivatives were fused with the GAL4 DNA-binding domain (BD) in *pGBKT7*. To investigate the interactions of SEU with methyltransferases, CDSs of *ATX1*, *SDG4*, *CaM KMT*, *CMT2*, *DDM1*, *ERF6*, *DRM2*, *MRG1*, *MRG2*, *NRP2*, *ORC1A*, *ORC1B*, *ROS3*, *SDG25*, *MET1*, and *REF6* (Baumbusch *et al*, 2001) were fused to the GAL4 AD in *pGADT7*. To verify the domains of SEU involved in interactions with SCR and SDG4, CDSs of *SCR* and *SDG4* were fused to the GAL4 BD in *pGBKT7*, and those of *SEU* and its derivatives were fused to the GAL4 AD in *pGADT7*. Primers used for generating Y2H constructs are listed in Appendix Table S1.

The resulting constructs were cotransformed into yeast (*Saccharomyces cerevisiae*) strain AH109. The presence of transgenes in yeast cells was confirmed by growth on plates containing solid synthetic defined (SD) media lacking leucine (Leu) and tryptophan (Trp) (SD/-2). To assess protein–protein interactions, the transformed yeast cells were spread on plates containing SD media lacking adenine (Ade), histidine (His), Leu, and Trp (SD/-4). Plates were incubated at 30°C, and protein–protein interactions were observed after 3 days.

Antibodies

The *SEU* CDS was amplified from the WT cDNA using gene-specific primers (Appendix Table S1). The PCR product was cloned into the *pMAL-c2X* vector to express the SEU-MBP fusion in *Escherichia coli* BL21 (DE3) cells. The recombinant proteins were used to raise polyclonal antibodies in mice.

Antibody for ChIP: anti-GFP (Abcam, ab290), anti-H3K4me (Abcam, ab8895), anti-H3K4me2 (Abcam, ab7766), anti-H3K4me3 (Abcam, ab8580), anti-H3K36me (Abcam, ab9048), and anti-H3K36me3 (Abcam, ab9050).

Antibody for Western blot: Anti-SCR (Santa Cruz, sc-12643), Anti-myc (Abmart, M20002L), Anti-HA (Abmart, M20003L), Anti-FLAG (Abmart, M20008L), Anti-GFP (YTHX, ZA009), Anti-MBP (BioLabs, E8032L).

RNA extraction, reverse transcription (RT), and RT-quantitative PCR (RT–qPCR) assays

To perform RT–qPCR analysis of *WOX5*, total RNA was extracted from approximately 5 mm long root tip sections of WT and mutant seedlings harvested at 5 DAG. Subsequently, cDNA was prepared from 2 μg total RNA using Superscript III reverse transcriptase (Invitrogen) and quantified on a Roche 480 cycler using the SYBR Green Kit (Takara). Expression levels of *WOX5* were normalized relative to *ACT7* expression. Statistical significance was evaluated with Student's *t*-test. Primers used for RT–qPCR analysis are listed in Appendix Table S1.

Western blot analysis

Seedlings were ground to a fine powder in liquid nitrogen and transferred to the extraction buffer [50 mM Tris–HCl (pH 7.5), 150 mM NaCl, 10 mM EDTA, 50 mM DTT, 2% (*v/v*) Nonidet P-40, and protease inhibitor cocktail (Roche)]. To perform western blot analysis, protein samples were boiled in sodium dodecyl sulfate (SDS) loading buffer for 5 min, separated by SDS–polyacrylamide gel electrophoresis (SDS–PAGE), and transferred to polyvinylidene fluoride (PVDF) membranes. Proteins of interest were detected using specific antibodies.

Co-immunoprecipitation (Co-IP) assays

To perform Co-IP assays, *p35S::SCR-GFP* and WT Col-0 seedlings were harvested at 5 DAG and homogenized in protein lysis buffer [50 mM Tris–HCl (pH 7.5), 150 mM NaCl, 5 mM EDTA, 0.1% Triton X-100, 0.2% Nonidet P-40, 0.6 mM phenylmethylsulfonyl fluoride (PMSF), 20 μM MG132, and protease inhibitor cocktail (Roche)]. After protein extraction, 20 μl protein A/G plus agarose

beads (Santa Cruz Biotechnology) was added to 2 mg protein extracts to reduce nonspecific immunoglobulin binding. After 1 h of incubation, the supernatant was transferred to a new tube. Then, anti-GFP antibody-bound agarose beads (Chromtek) were added to each reaction and incubated at 4°C for 4 h. Col-0 seedlings were used as a negative control. The precipitated samples were washed at least four times with the lysis buffer and then eluted by boiling the beads in SDS protein loading buffer for 5 min. SEU and GFP proteins were detected with anti-SEU antibody (1:2,000) and anti-GFP antibody (1:2,000), respectively.

Co-IP assays using *N. benthamiana* leaves were performed as described previously (Liu *et al*, 2010). *Agrobacterium tumefaciens* strain GV3101, carrying *p35S::SCR-GFP* and *p35S::SDG4-myc* constructs, or *p35S::SEU-GFP, p35S::SDG4-myc* and *p35S::SCR-HA* constructs, was infiltrated into tobacco leaves. The transformed *N. benthamiana* leaves were ground into a fine powder and transferred to the lysis buffer [50 mM Tris-MES (pH 8.0), 0.5 M sucrose, 1 mM MgCl$_2$, 10 mM EDTA, 5 mM DTT, 0.5 mM PMSF, 50 μM MG132, and protease inhibitor cocktail (Roche)]. The Co-IP procedure was the same as that described for *Arabidopsis*.

In vitro pull-down assays

To detect the SEU–SCR interaction using pull-down assays, SHR-FLAG and SCR-FLAG fusion proteins were synthesized by *in vitro* transcription/translation reactions (Promega). The SEU-MBP protein was affinity purified. Per reaction, 15 μl agarose beads bound by 1 μg SEU-MBP was incubated with 10 μl SHR-FLAG or SCR-FLAG protein in 1 ml reaction buffer [25 mM Tris–HCl (pH 7.5), 100 mM NaCl, 1 mM DTT, and protease inhibitor cocktail (Roche)] at 4°C for 1 h. The beads were then collected and washed three times with washing buffer [25 mM Tris–HCl (pH 7.5), 150 mM NaCl, and 1 mM DTT]. The bound proteins were eluted off the agarose beads using the elution buffer [25 mM Tris–HCl (pH 7.5), 100 mM NaCl, 1 mM DTT, and 10 mM maltose]. The SHR-FLAG and SCR-FLAG proteins were detected by western blotting using anti-FLAG antibody (1:2,000). Purified MBP was used as a negative control.

Transient expression assays in *Nicotiana benthamiana* leaves

The promoter of *WOX5* was amplified from the genomic DNA of Col-0 and cloned into the *pGreenII 0800-LUC* (Hellens *et al*, 2005) vector to generate a reporter construct. The *Renilla luciferase* (*REN*) gene under the control of the CaMV *35S* promoter was used as an internal control. To generate the effector constructs, CDSs of *SEU* and *SCR* were cloned into the *pUC19-35S-HA-RBS* vector (Li *et al*, 2005) under the control of the *35S* promoter. Primers used for vector construction are listed in Appendix Table S1. Firefly LUC and REN activities were measured using the Dual-LUC Reporter Assay System (Promega), according to the manufacturer's instructions.

Chromatin immunoprecipitation (ChIP)-qPCR assays

Root tips were harvested from seedlings at 5 DAG and crosslinked using 1% formaldehyde at room temperature for 10 min. The crosslinking reaction was stopped by the addition of 0.125 M glycine. The chromatin complex was isolated and resuspended in lysis buffer [50 mM HEPES (pH 7.5), 150 mM NaCl, 1 mM EDTA,

1% SDS, 1% Triton X-100, 0.1% sodium deoxycholate, 1 mM PMSF, and 1 × protease inhibitor cocktail (Roche)]. Then, the chromatin was sheared by sonication to an average size of approximately 200 bp. The sheared chromatin was pre-cleared with Protein A salmon sperm-coupled agarose (Millipore), and 10 μl of the pre-cleared chromatin was set aside for use as an input control. The remaining chromatin complex was immunoprecipitated overnight at 4°C with the following antibodies: anti-GFP, anti-H3K4me, anti-H3K4me2, anti-H3K4me3, anti-H3K36me, and anti-H3K36me3. The immunoprecipitated chromatin complex was washed once with each of the following buffers in this order: low-salt buffer [20 mM Tris–HCl (pH 8.0), 2 mM EDTA, 150 mM NaCl, 0.5% Triton X-100, and 0.2% SDS]; high-salt buffer [20 mM Tris–HCl (pH 8.0), 2 mM EDTA, 500 mM NaCl, 0.5% Triton X-100, and 0.2% SDS]; LiCl buffer [10 mM Tris–HCl (pH 8.0), 1 mM EDTA, 0.25 M LiCl, 0.5% NP-40, and 0.5% sodium deoxycholate]; and TE buffer [10 mM Tris–HCl (pH 8.0) and 1 mM EDTA]. After washing, the immunoprecipitated chromatin was eluted with elution buffer (1% SDS and 0.1 M NaHCO$_3$). The protein–DNA crosslinks were reversed by incubating the immunoprecipitated complexes at 65°C overnight. DNA was recovered using the QIAquick PCR Purification Kit (Qiagen). ChIP signals were quantified as the percentage of total input DNA and normalized relative to the control (*ACT7*). Primers used for qPCR are listed in Appendix Table S1.

Data availability

This study includes no data deposited in external repositories.

Expanded View for this article is available online.

Author contributions

XZ, HZ, and CL designed the research; HZ, XZ, YY, and LL performed the research; XZ, HZ, WZ, and CL analyzed the data; XZ, WZ, and CL wrote the paper; and CL conceived and supervised the study.

Conflict of interest

The authors declare that they have no conflict of interest.

References

Agulnick AD, Taira M, Breen JJ, Tanaka T, Dawid IB, Westphal H (1996) Interactions of the LIM-domain-binding factor Ldb1 with LIM homeodomain proteins. *Nature* 384: 270 – 272

Aichinger E, Kornet N, Friedrich T, Laux T (2012) Plant stem cell niches. *Annu Rev Plant Biol* 63: 615 – 636

Aida M, Beis D, Heidstra R, Willemsen V, Blilou I, Galinha C, Nussaume L, Noh YS, Amasino R, Scheres B (2004) The *PLETHORA* genes mediate patterning of the *Arabidopsis* root stem cell niche. *Cell* 119: 109 – 120

Bao F, Azhakanandam S, Franks RG (2010) *SEUSS* and *SEUSS-LIKE* transcriptional adaptors regulate floral and embryonic development in *Arabidopsis*. *Plant Physiol* 152: 821 – 836

Baumbusch LO, Thorstensen T, Krauss V, Fischer A, Naumann K, Assalkhou R, Schulz I, Reuter G, Aalen RB (2001) The *Arabidopsis thaliana* genome contains at least 29 active genes encoding SET domain proteins that can be assigned to four evolutionarily conserved classes. *Nucleic Acids Res* 29: 4319 – 4333

van den Berg C, Willemsen V, Hage W, Weisbeek P, Scheres B (1995) Cell fate in the *Arabidopsis* root meristem determined by directional signalling. *Nature* 378: 62 – 65

Berr A, Xu L, Gao J, Cognat V, Steinmetz A, Dong A, Shen WH (2009) SET DOMAIN GROUP25 encodes a histone methyltransferase and is involved in FLOWERING LOCUS C activation and repression of flowering. *Plant Physiol* 151: 1476 – 1485

Blilou I, Xu J, Wildwater M, Willemsen V, Paponov I, Friml J, Heidstra R, Aida M, Palme K, Scheres B (2005) The PIN auxin efflux facilitator network controls growth and patterning in *Arabidopsis* roots. *Nature* 433: 39 – 44

Bronstein R, Levkovitz L, Yosef N, Yanku M, Ruppin E, Sharan R, Westphal H, Oliver B, Segal D (2010) Transcriptional regulation by CHIP/LDB complexes. *PLoS Genet* 6: e1001063

Bronstein R, Segal D (2011) Modularity of CHIP/LDB transcription complexes regulates cell differentiation. *Fly* 5: 200 – 205

Cartagena JA, Matsunaga S, Seki M, Kurihara D, Yokoyama M, Shinozaki K, Fujimoto S, Azumi Y, Uchiyama S, Fukui K (2008) The *Arabidopsis* SDG4 contributes to the regulation of pollen tube growth by methylation of histone H3 lysines 4 and 36 in mature pollen. *Dev Biol* 315: 355 – 368

Chen H, Zou Y, Shang Y, Lin H, Wang Y, Cai R, Tang X, Zhou JM (2008) Firefly luciferase complementation imaging assay for protein-protein interactions in plants. *Plant Physiol* 146: 368 – 376

Chen Q, Sun J, Zhai Q, Zhou W, Qi L, Xu L, Wang B, Chen R, Jiang H, Qi J *et al* (2011) The basic helix-loop-helix transcription factor MYC2 directly represses *PLETHORA* expression during jasmonate-mediated modulation of the root stem cell niche in *Arabidopsis*. *Plant Cell* 23: 3335 – 3352

Cheng K, Xu Y, Yang C, Ouellette L, Niu L, Zhou X, Chu L, Zhuang F, Liu J, Wu H *et al* (2020) Histone tales: lysine methylation, a protagonist in *Arabidopsis* development. *J Exp Bot* 71: 793 – 807

Clark NM, Fisher AP, Berckmans B, Van denBroeck L, Nelson EC, Nguyen TT, Bustillo-Avendano E, Zebell SG, Moreno-Risueno MA, Simon R *et al* (2020) Protein complex stoichiometry and expression dynamics of transcription factors modulate stem cell division. *Proc Natl Acad Sci USA* 117: 15332 – 15342

Cruz-Ramirez A, Diaz-Trivino S, Blilou I, Grieneisen VA, Sozzani R, Zamioudis C, Miskolczi P, Nieuwland J, Benjamins R, Dhonukshe P *et al* (2012) A bistable circuit involving SCARECROW-RETINOBLASTOMA integrates cues to inform asymmetric stem cell division. *Cell* 150: 1002 – 1015

Cruz-Ramirez A, Diaz-Trivino S, Wachsman G, Du Y, Arteaga-Vazquez M, Zhang H, Benjamins R, Blilou I, Neef AB, Chandler V *et al* (2013) A SCARECROW-RETINOBLASTOMA protein network controls protective quiescence in the *Arabidopsis* root stem cell organizer. *PLoS Biol* 11: e1001724

De-La-Pena C, Rangel-Cano A, Alvarez-Venegas R (2012) Regulation of disease-responsive genes mediated by epigenetic factors: interaction of *Arabidopsis-Pseudomonas*. *Mol Plant Pathol* 13: 388 – 398

Di Laurenzio L, Wysocka-Diller J, Malamy JE, Pysh L, Helariutta Y, Freshour G, Hahn MG, Feldmann KA, Benfey PN (1996) The *SCARECROW* gene regulates an asymmetric cell division that is essential for generating the radial organization of the *Arabidopsis* root. *Cell* 86: 423 – 433

Ding Z, Friml J (2010) Auxin regulates distal stem cell differentiation in *Arabidopsis* roots. *Proc Natl Acad Sci USA* 107: 12046–12051

Dinneny JR, Benfey PN (2008) Plant stem cell niches: standing the test of time. *Cell* 132: 553–557

Dolan L, Janmaat K, Willemsen V, Linstead P, Poethig S, Roberts K, Scheres B (1993) Cellular-organization of the *Arabidopsis-thaliana* root. *Development* 119: 71–84

Forzani C, Aichinger E, Sornay E, Willemsen V, Laux T, Dewitte W, Murray JA (2014) WOX5 suppresses *CYCLIN D* activity to establish quiescence at the center of the root stem cell niche. *Curr Biol* 24: 1939–1944

Franks RG, Wang C, Levin JZ, Liu Z (2002) *SEUSS*, a member of a novel family of plant regulatory proteins, represses floral homeotic gene expression with *LEUNIG*. *Development* 129: 253–263

Fukaki H, Wysocka-Diller J, Kato T, Fujisawa H, Benfey PN, Tasaka M (1998) Genetic evidence that the endodermis is essential for shoot gravitropism in *Arabidopsis thaliana*. *Plant J* 14: 425–430

Galinha C, Hofhuis H, Luijten M, Willemsen V, Blilou I, Heidstra R, Scheres B (2007) PLETHORA proteins as dose-dependent master regulators of *Arabidopsis* root development. *Nature* 449: 1053–1057

Gallagher KL, Paquette AJ, Nakajima K, Benfey PN (2004) Mechanisms regulating SHORT-ROOT intercellular movement. *Curr Biol* 14: 1847–1851

Gong X, Flores-Vergara MA, Hong JH, Chu H, Lim J, Franks RG, Liu Z, Xu J (2016) SEUSS integrates gibberellin signaling with transcriptional inputs from the SHR-SCR-SCL3 module to regulate middle cortex formation in the *Arabidopsis* root. *Plant Physiol* 170: 1675–1683

Grigorova B, Mara C, Hollender C, Sijacic P, Chen X, Liu Z (2011) LEUNIG and SEUSS co-repressors regulate *miR172* expression in *Arabidopsis* flowers. *Development* 138: 2451–2456

Haecker A, Gross-Hardt R, Geiges B, Sarkar A, Breuninger H, Herrmann M, Laux T (2004) Expression dynamics of *WOX* genes mark cell fate decisions during early embryonic patterning in *Arabidopsis thaliana*. *Development* 131: 657–668

Heidstra R, Welch D, Scheres B (2004) Mosaic analyses using marked activation and deletionclones dissect *Arabidopsis* SCARECROW action in asymmetric cell division. *Genes Dev* 18: 1964–1969

Helariutta Y, Fukaki H, Wysocka-Diller J, Nakajima K, Jung J, Sena G, Hauser MT, Benfey PN (2000) The *SHORT-ROOT* gene controls radial patterning of the *Arabidopsis* root through radial signaling. *Cell* 101: 555–567

Hellens RP, Allan AC, Friel EN, Bolitho K, Grafton K, Templeton MD, Karunairetnam S, Gleave AP, Laing WA (2005) Transient expression vectors for functional genomics, quantification of promoter activity and RNA silencing in plants. *Plant Methods* 1: 13

Huai J, Zhang X, Li J, Ma T, Zha P, Jing Y, Lin R (2018) SEUSS and PIF4 coordinately regulate light and temperature signaling pathways to control plant growth. *Mol Plant* 11: 928–942

Jürgens G, Ruiz RAT, Laux T, Mayer U, Berleth T (1994) Early events in apical-basal pattern formation in *Arabidopsis*. In *Plant Molecular Biology: molecular-genetic analysis of plant development and metabolism*, Coruzzi G, Puigdomenech P (eds), pp 95–103. Berlin: Springer

Jürgens G (2001) Apical-basal pattern formation in *Arabidopsis* embryogenesis. *EMBO J* 20: 3609–3616

Kumpf R, Thorstensen T, Rahman MA, Heyman J, Nenseth HZ, Lammens T, Herrmann U, Swarup R, Veiseth SV, Emberland G *et al* (2014) The ASH1-RELATED3 SET-domain protein controls cell division competence of the meristem and the quiescent center of the *Arabidopsis* primary root. *Plant Physiol* 166: 632–643

Li X, Lin H, Zhang W, Zou Y, Zhang J, Tang X, Zhou JM (2005) Flagellin induces innate immunity in nonhost interactions that is suppressed by

Pseudomonas syringae effectors. *Proc Natl Acad Sci USA* 102: 12990–12995

Liu Z, Karmarkar V (2008) Groucho/Tup1 family co-repressors in plant development. *Trends Plant Sci* 13: 137–144

Liu L, Zhang Y, Tang S, Zhao Q, Zhang Z, Zhang H, Dong L, Guo H, Xie Q (2010) An efficient system to detect protein ubiquitination by agroinfiltration in *Nicotiana benthamiana*. *Plant J* 61: 893–903

Liu G, Dean A (2019) Enhancer long-range contacts: the multi-adaptor protein LDB1 is the tie that binds. *Biochim Biophys Acta Gene Regul Mech* 1862: 625–633

Long Y, Stahl Y, Weidtkamp-Peters S, Postma M, Zhou W, Goedhart J, Sanchez-Perez MI, Gadella TWJ, Simon R, Scheres B *et al* (2017) *In vivo* FRET-FLIM reveals cell-type-specific protein interactions in *Arabidopsis* roots. *Nature* 548: 97–102

Love PE, Warzecha C, Li L (2014) Ldb1 complexes: the new master regulators of erythroid gene transcription. *Trends Genet* 30: 1–9

Marhava P, Hoermayer L, Yoshida S, Marhavy P, Benkova E, Friml J (2019) Re-activation of stem cell pathways for pattern restoration in plant wound healing. *Cell* 177: 957–969

Matthews JM, Visvader JE (2003) LIM-domain-binding protein 1: a multifunctional cofactor that interacts with diverse proteins. *EMBO Rep* 4: 1132–1137

van Meyel DJ, Thomas JB, Agulnick AD (2003) Ssdp proteins bind to LIM-interacting co-factors and regulate the activity of LIM-homeodomain protein complexes *in vivo*. *Development* 130: 1915–1925

Morcillo P, Rosen C, Baylies MK, Dorsett D (1997) Chip, a widely expressed chromosomal protein required for segmentation and activity of a remote wing margin enhancer in *Drosophila*. *Genes Dev* 11: 2729–2740

Murashige T, Skoog F (1962) A revised medium for rapid growth and bio assays with tobacco tissue cultures. *Physiol Plantarum* 15: 473–497

Nakajima K, Sena G, Nawy T, Benfey PN (2001) Intercellular movement of the putative transcription factor SHR in root patterning. *Nature* 413: 307–311

Petricka JJ, Winter CM, Benfey PN (2012) Control of *Arabidopsis* root development. *Annu Rev Plant Biol* 63: 563–590

Pfluger J, Zambryski P (2004) The role of SEUSS in auxin response and floral organ patterning. *Development* 131: 4697–4707

Pi L, Aichinger E, van der Graaff E, Llavata-Peris CI, Weijers D, Hennig L, Groot E, Laux T (2015) Organizer-derived WOX5 signal maintains root columella stem cells through chromatin-mediated repression of *CDF4* Expression. *Dev Cell* 33: 576–588

Sabatini S, Beis D, Wolkenfelt H, Murfett J, Guilfoyle T, Malamy J, Benfey P, Leyser O, Bechtold N, Weisbeek P *et al* (1999) An auxin-dependent distal organizer of pattern and polarity in the *Arabidopsis* root. *Cell* 99: 463–472

Sabatini S, Heidstra R, Wildwater M, Scheres B (2003) SCARECROW is involved in positioning the stem cell niche in the *Arabidopsis* root meristem. *Genes Dev* 17: 354–358

Sarkar AK, Luijten M, Miyashima S, Lenhard M, Hashimoto T, Nakajima K, Scheres B, Heidstra R, Laux T (2007) Conserved factors regulate signalling in *Arabidopsis thaliana* shoot and root stem cell organizers. *Nature* 446: 811–814

Scheres B, Benfey PN (1999) Asymmetric cell division in plants. *Annu Rev Plant Physiol* 50: 505–537

Scheres B (2007) Stem-cell niches: nursery rhymes across kingdoms. *Nat Rev Mol Cell Biol* 8: 345–354

Shimotohno A, Heidstra R, Blilou I, Scheres B (2018) Root stem cell niche organizer specification by molecular convergence of PLETHORA and SCARECROW transcription factor modules. *Genes Dev* 32: 1085–1100

Sridhar VV, Surendrarao A, Gonzalez D, Conlan RS, Liu Z (2004) Transcriptional repression of target genes by LEUNIG and SEUSS, two interacting regulatory proteins for *Arabidopsis* flower development. *Proc Natl Acad Sci USA* 101: 11494–11499

Sridhar VV, Surendrarao A, Liu Z (2006) *APETALA1* and *SEPALLATA3* interact with *SEUSS* to mediate transcription repression during flower development. *Development* 133: 3159–3166

Stahl Y, Wink RH, Ingram GC, Simon R (2009) A signaling module controlling the stem cell niche in *Arabidopsis* root meristems. *Curr Biol* 19: 909–914

Stahl Y, Grabowski S, Bleckmann A, Kuhnemuth R, Weidtkamp-Peters S, Pinto KG, Kirschner GK, Schmid JB, Wink RH, Hulsewede A *et al* (2013) Moderation of *Arabidopsis* root sternness by CLAVATA1 and ARABIDOPSIS CRINKLY4 receptor kinase complexes. *Curr Biol* 23: 362–371

Tamada Y, Yun JY, Woo SC, Amasino RM (2009) *Arabidopsis* TRITHORAX-RELATED7 is required for methylation of lysine 4 of histone H3 and for transcriptional activation of flowering locus C. *Plant Cell* 21: 3257–3269

Weigel D, Jürgens G (2002) Stem cells that make stems. *Nature* 415: 751–754

Wysocka-Diller JW, Helariutta Y, Fukaki H, Malamy JE, Benfey PN (2000) Molecular analysis of SCARECROW function reveals a radial patterning mechanism common to root and shoot. *Development* 127: 595–603

Xu J, Hofhuis H, Heidstra R, Sauer M, Friml J, Scheres B (2006) A molecular framework for plant regeneration. *Science* 311: 385–388

Zhang Y, Jiao Y, Liu Z, Zhu YX (2015) ROW1 maintains quiescent centre identity by confining *WOX5* expression to specific cells. *Nat Commun* 6: 6003

Zhang X, Zhou W, Chen Q, Fang M, Zheng S, Scheres B, Li C (2018) Mediator subunit MED31 is required for radial patterning of *Arabidopsis* roots. *Proc Natl Acad Sci USA* 115: E5624–E5633

Zhou W, Wei L, Xu J, Zhai Q, Jiang H, Chen R, Chen Q, Sun J, Chu J, Zhu L *et al* (2010) *Arabidopsis* tyrosylprotein sulfotransferase acts in the auxin/PLETHORA pathway in regulating postembryonic maintenance of the root stem cell niche. *Plant Cell* 22: 3692–3709

Zhou W, Lozano-Torres JL, Blilou I, Zhang X, Zhai Q, Smant G, Li C, Scheres B (2019) A jasmonate signaling network activates root stem cells and promotes regeneration. *Cell* 177: 942–956